AD NUMBER

AD411164

LIMITATION CHANGES

TO:

Approved for public release; distribution is unlimited.

FROM:

**Distribution authorized to U.S. Gov't. agencies and their contractors;
Administrative/Operational Use; JUN 1963. Other requests shall be referred to Office of Naval Research, Arlington, VA 22203.**

AUTHORITY

ONR ltr dtd 4 May 1977

TYCO LABORATORIES, INC.
BEAR HILL, WALTHAM 54, MASSACHUSETTS
AREA CODE 617
TELEPHONE: 899-1650

ELECTROCHEMISTRY OF FUEL CELL ELECTRODES.

Kinetics of the Fe^{+++}/Fe^{++} Reaction on Fe-Cr Alloys

by

A. C. Makrides

Technical Memorandum No. 4

Contract No. Nonr-3765(00)

dated April 16, 1962
expiring April 15, 1963

ARPA Order No. 302-62
Project Code 9800
Task No. NR 359-443

June, 1963

prepared for:

OFFICE OF NAVAL RESEARCH
Materials Sciences Division
Washington 25, D. C.

ABSTRACT

The electrode kinetics of the $Fe^{(+++)}/Fe^{(++)}$ couple on passive Fe-Cr alloys were studied in acid solutions of constant ionic strength (M $MgSO_4$). Tafel behavior is generally observed with exchange currents of the order of 10^{-6} amp/cm^2 ($C_{Fe^{+++}} = C_{Fe^{++}} = 0.050M$), a cathodic transfer coefficient of 0.40, and an anodic transfer coefficient of 0.36. The electrochemical reaction order is unity both for oxidation of $Fe^{(++)}$ and reduction of $Fe^{(+++)}$; the heat of activation at the reversible potential is 10.8 kcal/mol.

The results show that an appreciable fraction (about 0.4) of the total potential drop on anodic polarization occurs within the passive film. This potential drop is probably associated with changes in the average oxidation state of cations between the inner and outer layers of the surface oxide. The electrochemical characteristics of the film depend on the pH of the solution, probably because of the migration of protons into the passive film. A change in the kinetics of $Fe^{(++)}$ oxidation which occurs in the transpassive region for the Fe-Cr alloy is probably due to the production of Fe^{+3} or $Cr^{(+6)}$ ions in the inner oxide layer.

* 10 to the -6th power

I. INTRODUCTION

The kinetics of the Fe^{+++}/Fe^{++} couple on superficially oxidized electrodes present a number of interesting features[1-4]. In general, the exchange currents are low ($\sim 10^{-6}$ a/cm^2), the transfer coefficients have unusual values and sums less than unity, and the anodic and cathodic curves are generally asymmetrical[1-4]. These features appear to be basic to an electrode covered with a thin oxide (i.e., a passive electrode) and not to be related to the specific nature of the redox couple. They are probably connected with electronic processes within the surface oxide and are expected, therefore, to occur with any redox reaction taking place at such an electrode[4]. In particular, they undoubtedly play a major role in oxygen evolution and reduction on electrodes which form surface oxides in the relevant potential region.

A study of the kinetics of the Fe^{+++}/Fe^{++} reaction on passive Fe, Ni, and Ti electrodes was presented in a previous communication[4]. This redox couple was chosen as a model reaction because its kinetics are straight-forward on oxide-free electrodes[5, 6] and because both oxidation of Fe^{++} and reduction of Fe^{+++} can be followed over a relatively wide potential range.

A detailed study of the redox kinetics of the Fe^{+++}/Fe^{++} reaction on Fe-Cr alloys is presented here. These alloy electrodes, which show the same general features as other superficially oxidized electrodes, are convenient experimentally since they have small dissolution rates in acid solutions. In addition to the usual experimental quantities required for a more or less complete characterization of a redox reaction (Tafel parameters, reaction order, pH dependence, and temperature coefficient), the dependence of the kinetics on the electrochemical conditioning of the surface film (e.g., "deforming") was also determined.

II. EXPERIMENTAL

The electrolytic cell, measuring circuits, and experimental procedure were described previously[4, 7]. Galvanostic measurements were generally employed. Under all experimental conditions, the diffusion-limited

current for either Fe^{++} or Fe^{+++} was at least one order of magnitude greater than the applied current[4]. Constant potential measurements were carried out with an electronic potentiostat similar to the one described by Gerischer and Staubach[8].

Fe-Cr alloys, prepared from electrolytic iron and electrolytic chromium, had as the main constituents 13.17% Cr, 0.008% C, 0.011% S, and the balance Fe. A limited amount of work was also done with a commercially available alloy (12.4 Cr, 0.44 Mn, 0.24 Ni and 0.12 % Cu).

The solution was M in $MgSO_4$. The large excess of bivalent, inert electrolyte insured a constant composition of the electrolytic double layer even at the highest concentration of Fe^{+++} and Fe^{++} ions. Reagents were of C.P. grade.

In general, potentials were measured both against a platinized Pt electrode in the same solution with the working electrode and a SCE electrode. Platinized Pt was reversible to Fe^{+++}/Fe^{++} as shown by its response to (Fe^{++}) or (Fe^{+++}) at fixed ionic strength (see, for example, Fig. 1) and its behavior upon polarization at a few μa in either direction. The reversible potential of the Fe^{+++}/Fe^{++} couple is pH-dependent because of equilibria involving $Fe(OH)^{++}$ and possibly $Fe(OH)^{+}$ [9]. The pH dependence of a platinized Pt electrode at a fixed $(Fe^{+++})/(Fe^{++})$ and fixed ionic strength (M $MgSO_4$) is shown in Fig. 2. The potentials in Figs. 1 and 2 include an appreciable liquid junction potential, which is, however, constant and independent of the (Fe^{+++}) and (Fe^{++}) concentrations and of the pH.

The concentrations of (Fe^{++}) and (Fe^{+++}) were determined by titration with $K_2Cr_2O_7$ in the standard way using diphenyl amine sodium sulfonate as the end-point indicator.

III. RESULTS

Reproducibility

Tafel curves were obtained for the Fe^{+++}/Fe^{++} reaction on Fe-Cr electrodes as was the case with passive Fe, Ni, and Ti electrodes[4]. Typical polarization curves for Fe-Cr are shown in Fig. 3. The anodic polarization curve was not semilogarithmic under certain conditions, but showed a more

complicated behavior described in detail below.

In general, the potential assumed a steady value within a short time after the current was set to a new value. Overshoot or undershoot, depending on whether the current was increasing or decreasing, was observed in certain potential ranges. These cases are discussed below.

The reproducibility of current-potential curves obtained with a given electrode over extended periods (~100 hrs.) is illustrated in Table I. The initial slow change, which comes to an end after about 24 hrs., is probably due to a change in the film. The rest-potential, which is originally about -20 mv vs. the reversible Fe^{+++}/Fe^{++} potential, slowly changes towards zero indicating a continuously diminishing contribution from corrosion reactions. The rest potential is within 3-5 mv of the reversible potential after about 24 hrs. in almost all of the solutions used here. In general, the electrodes were extremely stable after the first 24 hrs. and showed little susceptibility to poisoning. This is probably due in part to the smaller tendency of oxide-covered surfaces, as compared to oxide-free surfaces, for adsorbing impurities and in part to the relatively high, positive electrode potential.

Reaction Orders

Current-potential curves in a solution of constant pH and M in $MgSO_4$ were determined for (Fe^{++}) and (Fe^{+++}) concentrations between 0.01 and 0.06 M. The currents at a fixed anodic (0.60 V vs. SCE) and fixed cathodic (0.20V vs. SCE) potentials are shown in Fig. 4. Both electrochemical reaction orders

$$\left(\frac{\partial \log i_a}{\partial \log(Fe^{++})}\right)_{E_a} = 1 = \left(\frac{\partial \log i_c}{\partial \log(Fe^{+++})}\right)_{E_c} \qquad (1)$$

are equal to unity in solutions containing a large excess of inert electrolyte (M $MgSO_4$).

Temperature Coefficient

The temperature dependence of i_o, determined by extrapolation of

Table I

Oxidation of Fe^{++} (*)

t (hrs)	i_o (amp/cm^2)	b (v)	Rest Potential
2	5.0×10^{-7}	0.190	-0.022
24	3.8×10^{-7}	0.161	-0.006
80	3.8×10^{-7}	0.159	-0.001
120	4.0×10^{-7}	0.156	-0.0005

(*) $C_{Fe^{++}} = C_{Fe^{+++}} = 0.050$ M; M $MgSO_4$; pH = 0.30

of the cathodic Tafel line, in solutions of pH = 1.50 and 0.30 is shown in Fig. 5. The energy of activation is essentially independent of pH and is $\triangle H^* = 10.8$ kcal/mol.

Corrosion Reactions

The rest potential is negative to the Fe^{+++}/Fe^{++} reversible potential in solutions of low pH and low in (Fe^{+++}) or (Fe^{++}) indicating that the corrosion current is significant in comparison to i_o. In these cases, the polarization curves were corrected for the steady-state corrosion current by assuming that the latter was independent of the potential as it is known to be from potentiostatic measurements in the absence of the redox couple. The corrosion current was obtained from the anodic current required to polarize the electrode from its rest potential to the Fe^{+++}/Fe^{++} reversible potential. The curves were then corrected by subtracting this quantity from the anodic applied current and adding it to the cathodic applied current as shown in Fig. 6 for the commercial Fe-Cr alloy. The assumption of constancy of i_{corr} was checked by comparing i_{corr} determined as described above with the value calculated from the difference between the corrected cathodic curve and the corrected anodic curve extrapolated to the rest potential. Table II shows that values of i_{corr} obtained in these two ways agree closely.

pH Dependence

The exchange current and the Tafel slopes decrease with decreasing pH as shown in Fig. 7. The exchange current at pH = 1.35 is less than that at pH = 2.2 by a factor of about 3. This decrease is probably connected with changes in the concentration of ionic species in solution (e.g. $Fe(H_2O)^{+++}$, $Fe(OH)^{++}$, $Fe(OH)^{+}$, etc.) which are also responsible for the change of the reversible potential with pH.

At pH of 1.5 or less, a qualitative change in the anodic polarization curve can be induced by a brief cathodic pulse or may appear spontaneously after the electrode has been in solution for some time. This is described in detail below.

Table II

Corrosion Currents of Commercial Fe-Cr Alloy
N H_2SO_4 at 30°C

Fe^{++} (M/l)	Fe^{+++} (M/l)	E_{corr} (V)	i_{corr} (1) (a/cm^2)	$(i_c - i_a)$ at Ecorr (2) (a/cm^2)
1.09×10^{-3}	1.38×10^{-2}	-0.026	4.0×10^{-7}	3.3×10^{-7}
1.09×10^{-3}	2.83×10^{-2}	-0.025	4.2×10^{-7}	3.6×10^{-7}
1.09×10^{-3}	4.92×10^{-2}	-0.020	4.0×10^{-7}	3.2×10^{-7}
1.09×10^{-3}	6.94×10^{-2}	-0.018	5.0×10^{-7}	4.6×10^{-7}
2.07×10^{-3}	6.94×10^{-2}	-0.014	4.5×10^{-7}	4.0×10^{-7}
4.05×10^{-3}	6.94×10^{-2}	-0.013	3.0×10^{-7}	3.5×10^{-7}
5.90×10^{-3}	6.94×10^{-2}	-0.010	4.3×10^{-7}	3.0×10^{-7}

(1) Applied anodic current for $\eta = 0$

(2) From extrapolated polarization curves after corrections for i_{corr}.

"Forming" and "Deforming" of the Surface Film

It was observed that in solutions of low pH, the anodic and cathodic curves did not extrapolate to a common i_o although the rest potential coincided with the reversible Fe^{+++}/Fe^{++} potential. In particular, the anodic curve appeared to consist of two Tafel lines, the lower one extrapolating to about the same i_o as the cathodic curve. This change from a single anodic Tafel line to the type of curve shown in Fig. 8 was delayed or was even absent if the film was formed in a solution of high pH and the pH was later adjusted to a lower value. Also, it proved possible to induce this change by a brief cathodic pulse and to reverse it by an anodic pulse. These phenomena are obviously related to changes in the composition or structure of the surface film. The term "deforming" is used here to denote the change produced by a cathodic pulse while "forming" refers to the change induced by an anodic pulse.

Polarization curves obtained with electrodes pulsed anodically or cathodically are shown in Fig. 8. The effect of a cathodic pulse on the cathodic polarization curve is slight. An anodic pulse displaces the cathodic curve in the direction of higher overpotentials, but the effect is relatively small. However, at overpotentials more negative than about -150 mv, the electrode potential at a fixed current density increases rapidly with time, a phenomenon not observed with electrodes which had not been pulsed.

The kinetics of oxidation of Fe^{++} are changed substantially both by cathodic and by anodic pulses. The anodic curve after "deforming" is no longer semilogarithmic but is approximately by two Tafel lines with a fairly sharp transition (Fig. 9). The cathodic pulse does not increase the corrosion rate since the reversible potential and the rest potential after deforming are still the same. Furthermore, the effects of a cathodic pulse are not transitory. Anodic curves obtained shortly after a cathodic pulse are the same as those obtained 100 hrs. later. The curves shown in Figs. 8 and 9 were obtained 24 hrs. after the pulse was applied.

Anodic pulses displace the anodic curve towards higher overpotentials and increase the Tafel slope to relatively high values. The effects of anodic of cathodic pulses are essentially independent of the previous history of the electrode, i.e., of the order in which the electrode was pulsed.

Transpassive Region

The potential was always kept within the passive region for the Fe-Cr alloy in the measurements described above. At high anodic potentials the alloy begins to dissolve again at a steady rate which depends on the potential. The onset of anodic dissolution in the transpassive region has a pronounced effect on the kinetics of oxidation of Fe^{++}. First, there is an overshoot of the potential on increasing the current and an undershoot when the current is decreased. Second, the Tafel slope for Fe^{++} oxidation decreases substantially in the transpassive region of the alloy (Fig. 10). It might appear at first that the increase in total current is due to the additional anodic current corresponding to metal oxidation. However, measurements of the anodic polarization curve in the absence of the redox couple show that the metal oxidation current is entirely negligible (Fig. 11). For example, at E = 0.850 vs. SCE (η = 0.425 V) the total current is 400 $\mu a/cm^2$, and the metal oxidation current is only 1.5 $\mu a/cm^2$.

IV. DISCUSSION

The low exchange currents and the unusual values of the Tafel slopes (see Table III) are characteristic features of redox reactions on superficially oxidized electrodes. In general, the sum of the apparent transfer coefficients on passive electrodes is less than unit. For example, Table III shows that $\alpha_a + \alpha_c = 0.76 \pm 0.03$ on Fe-Cr alloys; similar results were reported for other passive electrodes (1, 4). The parameters are in contrast to those obtained on oxide-free electrodes. For example, the exchange current on Pt electrodes with $C_{Fe^{+++}} = C_{Fe^{++}} = 0.05M$ is 1.5×10^{-2} A/cm^2 and the transfer coefficients are $\alpha_a = 0.58 \pm 0.02$ for the anodic and $\alpha_c = 0.42 \pm 0.02$ for the cathodic reaction (5, 6). The main difference in the kinetics (aside from difference of the exchange current) is in the apparent transfer coefficient for the anodic reaction. The cathodic transfer coefficients on passive Fe-Cr and on passive Ni and Ti (4) are all about the same as on Pt(*). The result $\alpha_a + \alpha_c < 1.0$ on passive electrodes is due to the smaller value of α_a on these electrodes and indicates that the anodic reaction is not a simple electrochemical process as it is on Pt.

(*) A cathodic transfer coefficient of 0.69 is observed for Fe^{+++} reduction on passive Fe(4). However, in this case the ionic current on cathodic polarization is probably a large fraction of the total current.

Table III

Fe^{+++}/Fe^{++} on Passive Fe-Cr
T = 30.0°C

Fe^{+++} (M/)	Fe^{++} (M/)	pH[1]	α_c	α_a
5.0×10^{-3}	5.0×10^{-3}	0.30	0.40	0.37
5.0×10^{-2}	5.0×10^{-2}	0.30	0.38	0.37
1.0×10^{-1}	1.0×10^{-1}	1.35	0.43	0.36
5.0×10^{-2}	5.0×10^{-2}	1.5	0.40	0.35
1.0×10^{-1}	1.0×10^{-1}	1.7	0.41	0.35
1.0×10^{-1}	1.0×10^{-1}	2.1	0.38	0.30
1.4×10^{-2}	5.0×10^{-3}	0.60[2]	0.42	0.38
4.1×10^{-2}	5.0×10^{-3}	0.60[2]	0.40	0.38
5.0×10^{-2}	5.0×10^{-2}	0.30	0.40	0.58[3]
5.0×10^{-2}	5.0×10^{-2}	1.35	0.42	0.37 0.58[3]

Avg. $\alpha_c = 0.40 \pm 0.01$

$\alpha_a = 0.36 \pm 0.02$

(1) All solutions M in $MgSO_4$ except where noted.

(2) No $MgSO_4$ added

(3) Two Tafel slopes on anodic polarization; data not included in average α_c or α_a.

It should be pointed out that in other respects the electrode behavior of passive metals towards the Fe^{+++}/Fe^{++} couple is similar to that of an inert electrode. Thus, the rest potential generally coincides with the reversible Fe^{+++}/Fe^{++} potential, a result which implies that the surface oxide film has a reasonable electronic conductivity. Also, passive electrodes respond to changes in the concentration of either (Fe^{++}) or (Fe^{+++}) in the simple way expected for a first order, one-electron reaction without the complications usually associated with specific adsorption of either ion. Thus, the electrochemical reaction order is unity provided sufficient excess of inert electrolyte is present to suppress effects arising from the diffuse part of the double layer. In less concentrated salt solutions, the composition of the double layer is not independent of the (Fe^{+++}) or (Fe^{++}) concentration and the kinetics are more complicated.

Ionic and Electronic Currents

The anodic reaction on passive electrodes involves probably both oxidation of the metal and oxidation of Fe^{++}. Therefore, the total applied current is the sum of an ionic current corresponding to the formation or reduction of the surface film, and of an electronic current equivalent to the rate at which the redox reaction is taking place. When no external current is applied, the anodic ionic current is equal to the net reduction current of Fe^{+++} at the resting potential. If the ionic current is appreciable, the rest potential is negative to the reversible potential (a mixed potential). If, however, the ionic current is negligible in comparison to the exchange current for the Fe^{+++}/Fe^{++} couple, the reversible and rest potentials coincide and the alloy functions essentially as an inert, indicator electrode.

The kinetics of film growth may be involved in determining the polarization curves either directly through the contribution of the ionic current to the total current, or indirectly through the possible effect of changes of film thickness and composition on the distribution of the total potential drop between the film and the electrolytic double layer. The commonly accepted account of the kinetics of growth of passive films is due to Vetter(10) who assumed that the rate-determing step is the field-assisted migration of cations through the oxide. In the steady state, film growth is balanced by

film dissolution which occurs by a purely chemical reaction. If the potential is raised to a more positive value, the film thickens until the field across it is reduced to its prior value; the rate of growth is then again equal to the dissolution rate. This mechanism accounts for the most notable characteristic of passive electrodes, namely a steady-state, oxidation current which is independent of potential. The most important aspects of this mechanism which bear on the present studies are the constant dissolution rate and the exponential dependence of the rate of film growth on the field across the oxide.

Consider a passive Fe-Cr electrode in a solution 0.05M in Fe^{+++} and Fe^{++} ions in $MgSO_4$, and of pH = 1.5. The steady state dissolution rate of the alloy is less than 10^{-7} a/cm^2, which is negligible in comparison to the exchange current. The distribution of potential from metal to electrolyte at the reversible Fe^{+++}/Fe^{++} potential may be described by

$$E_{rev} = V + E_{dl} = \text{Constant} \qquad (2)$$

where V is within the oxide, and E_{dl} is a potential drop across the oxide/electrolyte interface. If the electrode is polarized anodically, say to a potential E, an ionic and an electronic current flow across the film. The former corresponds to the rate of growth of the oxide and the latter to the rate of oxidation of Fe^{++}. As the film thickens, the ionic current eventually decreases to its previous value, i.e., 10^{-7} --10^{-8} a/cm^2. The electronic current depends on the kinetics of ferrous oxidation and is given by

$$i_a = i_o \exp(\beta_r \eta_{dl}) \qquad (3)$$

where η_{dl} is in units of RT/F, and α_r is the transfer coefficient for Fe^{++} oxidation.

The results show that in all cases studied (see also ref. 4) an appreciable fraction of the applied potential on anodic polarization is across the film. This implies that the transfer of electrons from the oxide/solution interface to the metal -- or of holes in the opposite direction -- occurs over a potential barrier. If it is assumed that the potential drop across the film is

a constant fraction, say γ, of the total applied potential, and since

$$\eta = E - E_{rev} = \Delta V + \eta_{dl} = \gamma\eta + \eta_{dl} \quad (4)$$

then the fraction of the overpotential across the double layer is

$$\eta_{dl} = (1 - \gamma)\eta \quad (5)$$

Substituting in Eq. (3) we have for the anodic current

$$i_a = i_o \exp\left[\beta_r (1 - \gamma)\eta\right] \quad (6)$$

On the other hand, the transfer of electrons from metal to the oxide/solution interface is apparently accompanied by a negligible change in the total potential drop across the film, and consequently

$$i_c = i_o \exp(-\alpha_r \eta_{dl}) = i_o \exp(-\alpha_r \eta) \quad (7)$$

where α_r is the transfer coefficient for Fe^{+++} reduction ($\alpha_r + \beta_r = 1$).

The sum of the apparent transfer coefficients is

$$\alpha_a + \alpha_c = (1 - \gamma)\beta_r + \alpha_r = 1 - \gamma\beta_r \quad (8)$$

so that in the particular case of Fe-Cr alloys ($\alpha_a + \alpha_c = 0.76$) γ is 0.4.

An alternative interpretation of the unusual transfer coefficients may be considered. If it is assumed that the transfer of electrons across the film gives rise to a potential drop, V_f, according to the dual barrier model proposed for redox reactions on valve metals, e.g. Zr (11), then the anodic current across the film may be expressed by

$$i_a = i_{o,f} \exp(\alpha_f V_f) \quad (9)$$

where the subscript f refers to the film. The current across the double layer is, of course, the same and is given by Eq. (8), while the total potential drop from metal to solution is again $\eta = V_f + \eta_{dl}$. Although the polarization curve defined by Eqs. (8) and (9) is not semilogarithmic, it may be approximated by a Tafel curve over a narrow range of current densities (11). It is difficult to decide on the basis of the polarization characteristics alone (the range of accessible current densities being relatively small) whether the dual-barrier model or the one advance above is applicable. However, the electrochemical reaction orders can be used to differentiate between these two alternative interpretations. According to the dual-barrier model, the reaction order is

$$\left(\frac{\partial \ln i}{\partial \ln C}\right)_E = \frac{\alpha_f}{\alpha_f + \beta_r} \qquad (10)$$

On the other hand, the account given above requires that

$$\left(\frac{\partial \ln i}{\partial \ln C}\right)_E = 1 \qquad (11)$$

since V, and consequently η_{dl}, are constant at constant E. The experimental results agree with Eq. (11) and show that the transfer of electrons across the film is not described by Eq.(9).

It should be noted that the postulated potential drop within the oxide film does not appear in the expression for the electrode potential when the Fe^{+++}/Fe^{++} is at equilibrium. The argument here parallels the analysis which shows that the thermodynamic potential of any redox couple is independent of the actual potential drop across the solid/electrolyte interface of an inert, indicator electrode. Similarly, the experimental results on anodic polarization do not refer to the absolute magnitude of potential drop within the oxide, but rather to changes of this potential.

The electronic properties of the surface oxide which give rise to the observed behavior may be described in terms of the continuum properties of

semiconducting oxides, e.g., it may be supposed that the oxide next to the solution is of p-type while that next to the metal is of n-type. However, it is doubtful that these terms are relevant since the thickness of the oxide is of the order of 100Å. Therefore, it is preferable to consider charge transfer within the oxide in terms of changes in chemical composition which may occur as the potential is changed to more or less positive values.

Consider, for example, a surface film of iron oxide in which the layers next to the solution are essentially Fe_2O_3, while the layers next to the metal may approach FeO. On cathodic polarization, an electron is transferred to a ferric ion in solution and a higher valency ion is left behind. The higher valency ion can accept an electron from a ferrous ion in the film which is in turn oxidized to the +3 state and eventually accepts an electron from the metal. On anodic polarization, an electron is transferred from a ferrous ion in solution to either a ferric ion in the film or to an ion of a higher valence, say Fe^{+4}, which may be associated with a cation vacancy. Further charge transfer must occur by transfer of an electron to a ferrous ion in the inner layer or by transfer to a ferric ion which may be produced next to the metal. Since the first alternative is not likely, transfer will depend on the production of ferric ions in the inner layer. This is associated with an overpotential which apparently constitutes an appreciable fraction of the total applied potential difference. A similar analysis is applicable to other oxide films (e.g. NiO) present on passive metals (4). The fraction of the overpotential which appears within the film is large in the case of Ti (0.60) and Fe-Cr (0.40), but is relatively small (0.15) in the case of Ni(4). In the case of Fe and Ti, and under circumstances previously discussed(4), practically all of the potential drop occurs in the oxide. In these cases, a substantial increase of the thickness of the oxide film apparently takes place on anodic polarization.

Changes of Film Characteristics

The electrochemical characteristics of the surface oxide are changed either by an anodic or cathodic pulse. Furthermore, they are obviously also different in the transpassive region of the alloy. A change in the anodic polarization curve once a certain overpotential was exceeded was previously reported by Stern (1) who tentatively attributed it to the onset of oxygen

evolution. The present study shows that oxygen evolution cannot be involved since the potential is in all cases less than the reversible oxygen potential.

The change of slope in the transpassive region is probably connected with the introduction into the film of large numbers of ions of higher valence (Fe^{+3}, Cr^{+6}). The potential drop within the oxide in the transpassive region apparently increases much more slowly with the total potential. As long as the metal oxidation current is negligible in comparison to the oxidation of Fe^{++}, the total i-E characteristics should approach that for the anodic oxidation of Fe^{++}. In particular, the apparent transfer coefficient should approach 0.60. The observed change in the Tafel slope is in the expected direction.

The effects of anodic and cathodic pulses suggest that the potential drop across the oxide changes after a pulse. Stated differently, these results suggest that the electronic characteristics of the oxide are altered substantially by pulsing. A cathodic pulse apparently decreases the fraction of the potential drop which is across the oxide; an anodic pulse has the opposite effect. The apparent anodic transfer coefficient changes accordingly towards larger or smaller values. The origin of this effect is not clear at present. It may be connected with migration of protons into or out of the film since a change similar to that produced by a cathodic pulse also occurs when the pH is lowered (12). Apparently, proton migration is a slow process since the changes produced by pulsing persist for at least 100 hours after the pulse. This conclusion is supported by the observation that the characteristics of a film formed in a solution of high pH remain the same for some time after the pH is adjusted to a lower value.

V. SUMMARY AND CONCLUSIONS

(1) Passive Fe-Cr alloy electrodes function as inert, indicator electrodes for the Fe^{+++}/Fe^{++} couple. The steady-state, ionic current is generally negligible compared with the electron current.

(2) Tafel curves are obtained on both anodic and cathodic polarization. The transfer coefficients are 0.36 for the anodic and 0.40 for the cathodic reaction. The exchange current is of the order of 10^{-6} a/cm^2 for $C_{Fe^{+++}}$

= $C_{Fe^{+++}}$ = 0.05M. The electrochemical reaction orders are unity for both Fe^{++} and Fe^{+++}. The temperature coefficient of the exchange current is 10.8 kcal/mol.

(3) The polarization characteristics suggest that an appreciable fraction of the total potential drop between electrode and solution is across the surface film. The potential drop across the film increases linearly with the total applied potential. This dependence leads to an apparent transfer coefficient for the anodic reaction which is substantially less than what is expected for the oxidation of Fe^{++}.

(4) The electrochemical characteristics of the passive film depend on the pH and can be modified by anodic or cathodic pulses. The film characteristics are also changed significantly when the potential is within the transpassive region for the alloy.

REFERENCES

1 Stern, M., J. Electrochem. Soc., 104, 559, 600 (1957)

2 Posey, F. A., J. Electrochem. Soc., 106, 582 (1959)

3 Makrides, A. C. and Stern, M., J. Electrochem. Soc., 107, 877(1960)

4 Makrides, A. C., submit., J. Electrochem. Soc.

5 Gerischer, J. Z. Elektrochem., 54, 362 (1950)

6 Randles, J. E. B., and Somerton, K. W., Trans. Faraday Soc., 48, 937 (1952).

7 Makrides, A. C., J. Electrochem., 109, 977 (1962)

8 Gerischer, H. and Staubach, K. E., Z. Elektrochem., 61, 789 (1957)

9 Latimer, W. M., "Oxidation Potentials", Prentice-Hall, 1952, p. 224

10 Vetter, K. J., Z. Elektrochem., 58, 230 (1954); 59, 67 (1955)

11 Meyer, R. E., J. Electrochem. Soc., 107, 847 (1960)

12 Leach, J. S. L., J. Inst. Met. 27,(1959)

FIGURE CAPTIONS

Fig. 1 The potential of platinized Pt as a function of the ferrous ion concentration at fixed ionic strength (M $MgSO_4$) and fixed ferric ion concentration and at 30^oC.

Fig. 2 The potential of platinized Pt at fixed $C_{Fe^{+++}}/C_{Fe^{++}}$ (0.05M) and fixed ionic strength (M $MgSO_4$) as a function of pH at 30^oC.

Fig. 3 Polarization curves of the Fe^{+++}/Fe^{++} couple (0.050M) on passive Fe-Cr in M $MgSO_4$ at pH = 2.2. The solid circles are calculated from $i_o = i_c \pm i_{appl}$ where i_c is the extrapolated cathodic current and i_{appl} the externally applied current (30^oC).

Fig. 4 The current at a fixed potential as a function of the concentration of ferrous or ferric ions -○- oxidation of Fe^{++} at 0.600 V vs. SCE -●- reduction of Fe^{+++} at 0.200 V vs. SCE (30^oC).

Fig. 5 The temperature coefficient of the exchange current (extrapolated from the cathodic curve) for Fe^{+++}/Fe^{++} (0.50M) in M $MgSO_4$.

Fig. 6 Current-potential curves for the Fe^{+++}/Fe^{++} couple (0.05M) on commercial Fe-Cr alloys. The full circles are obtained after correction for the corrosion current (30^oC).

Fig. 7 Polarization curves of the Fe^{+++}/Fe^{++} couple (0.10M) on passive Fe-Cr in M $MgSO_4$ at different pH (30^oC).

Fig. 8 The effect of anodic (●) and cathodic (○) pulsing on the polarization curve of the Fe^{+++}/Fe^{++} couple (0.10M) on passive Fe-Cr in M $MgSO_4$ at pH = 1.35. The curve corresponding to -◑- was obtained with electrodes which had not been pulsed (30^oC).

FIGURE CAPTIONS - continued

Fig. 9 The anodic polarization curve for Fe^{++} oxidation on passive Fe-Cr alloy after cathodic pulsing. Measurements were made 24 hrs. after pulsing.

Fig. 10 The anodic polarization curve for Fe^{++} (0.050M) oxidation in M $MgSO_4$ at pH = 0.30. Note the change in slope in the transpassive region ($\eta > 0.35$V or $E > 0.70$ V vs. SCE) ($30^{o}C$).

Fig. 11 The potentiostatic anodic polarization curve of Fe-Cr electrodes in M $MgSO_4$ at pH = 0.30 and at $30^{o}C$.

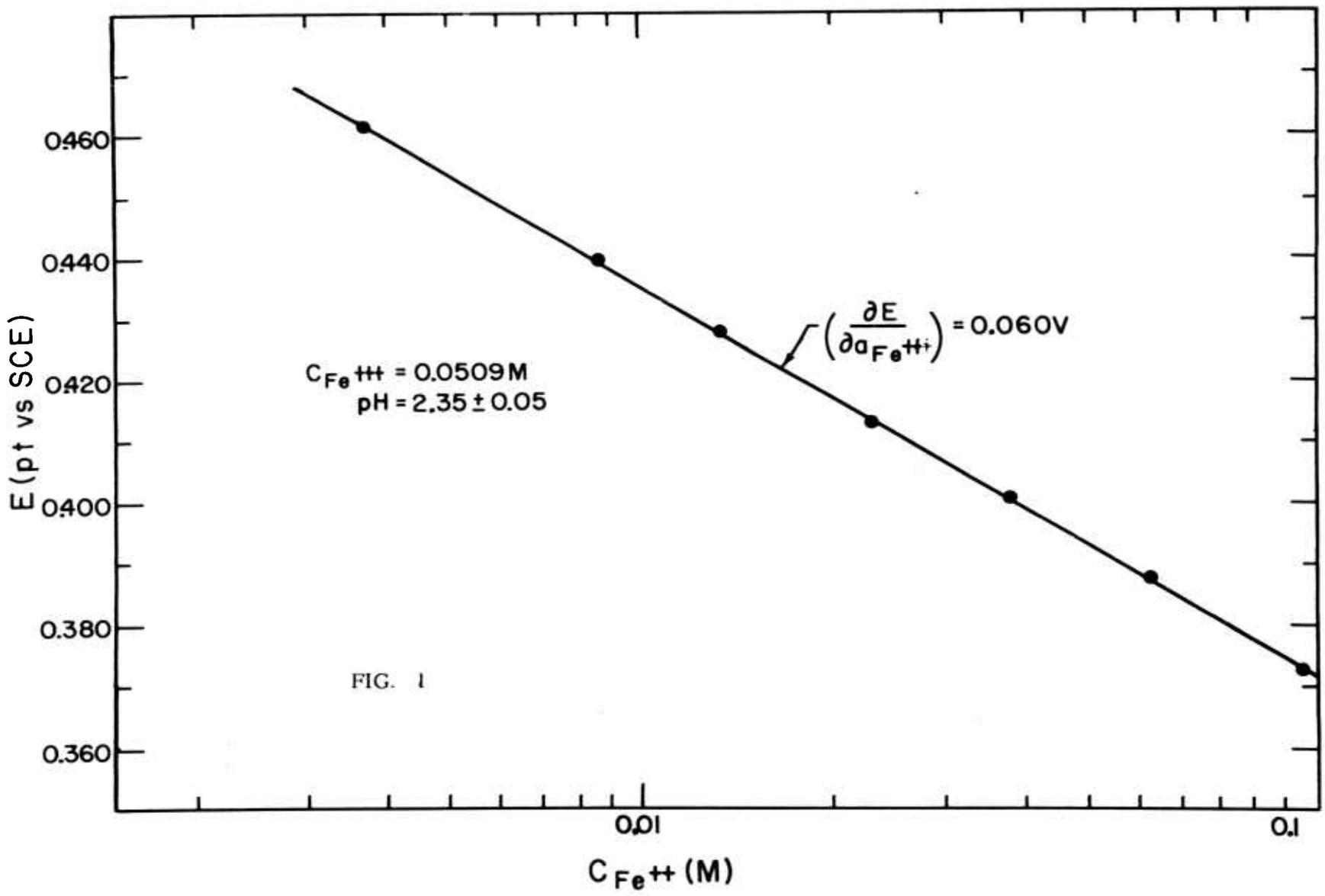
0.460
0.440
0.420
0.400
0.380
0.360
E (pt vs SCE)
$C_{Fe^{+++}}$ = 0.0509 M
pH = 2.35 ± 0.05
$\left(\frac{\partial E}{\partial a_{Fe^{+++}}}\right)$ = 0.060V
0.01
0.1
$C_{Fe^{++}}$ (M)

FIG. 1

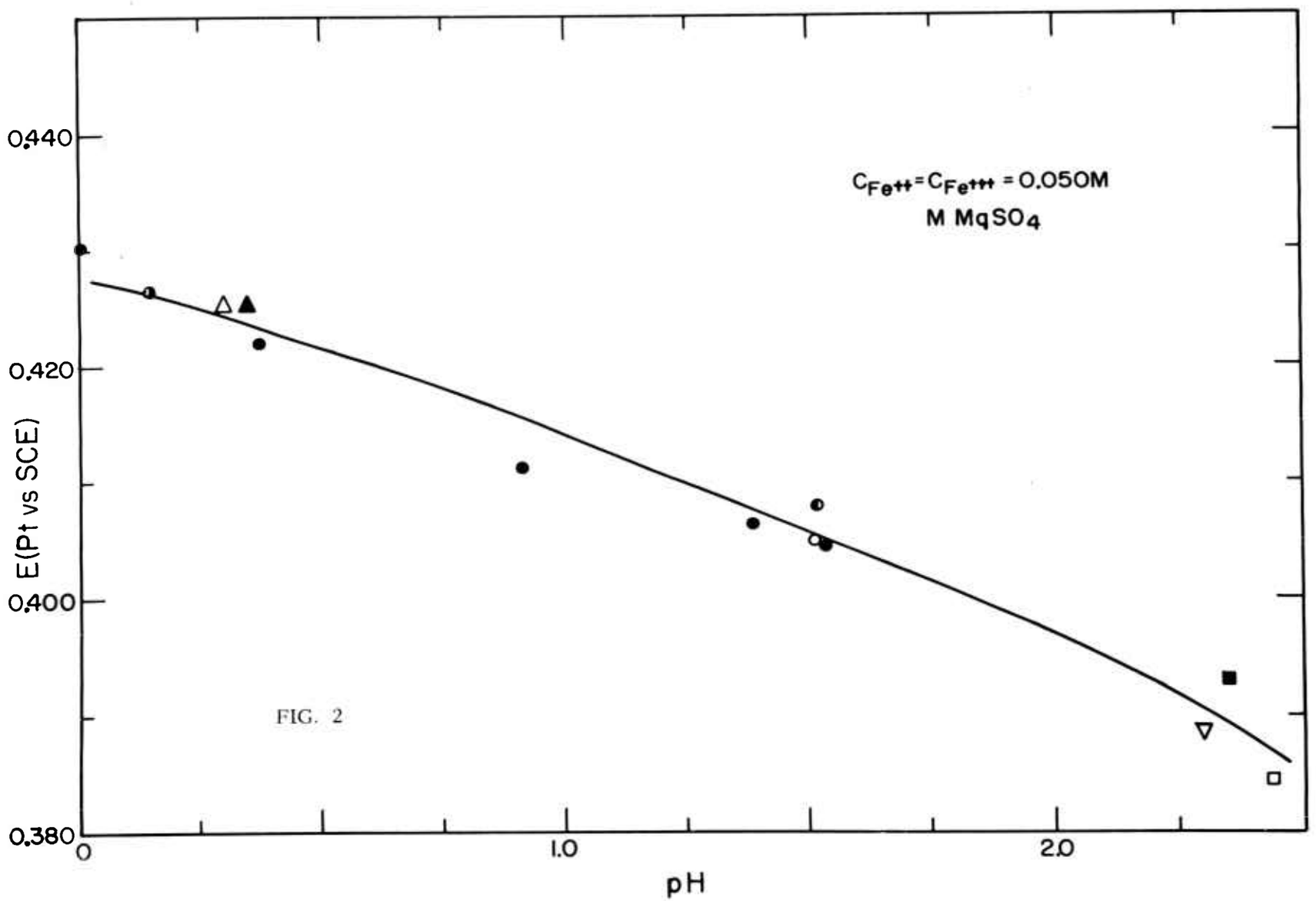

FIG. 2

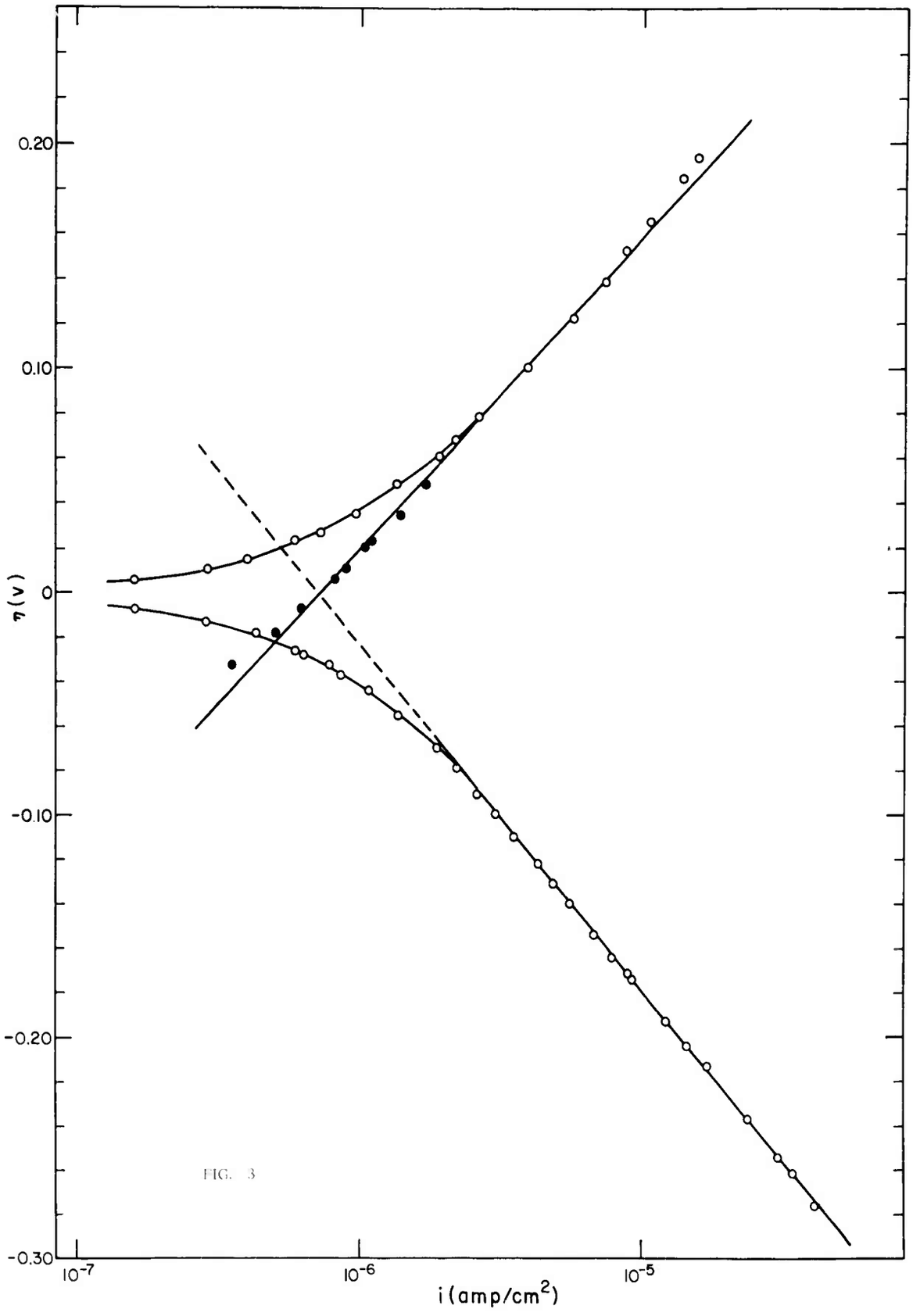

FIG. 3

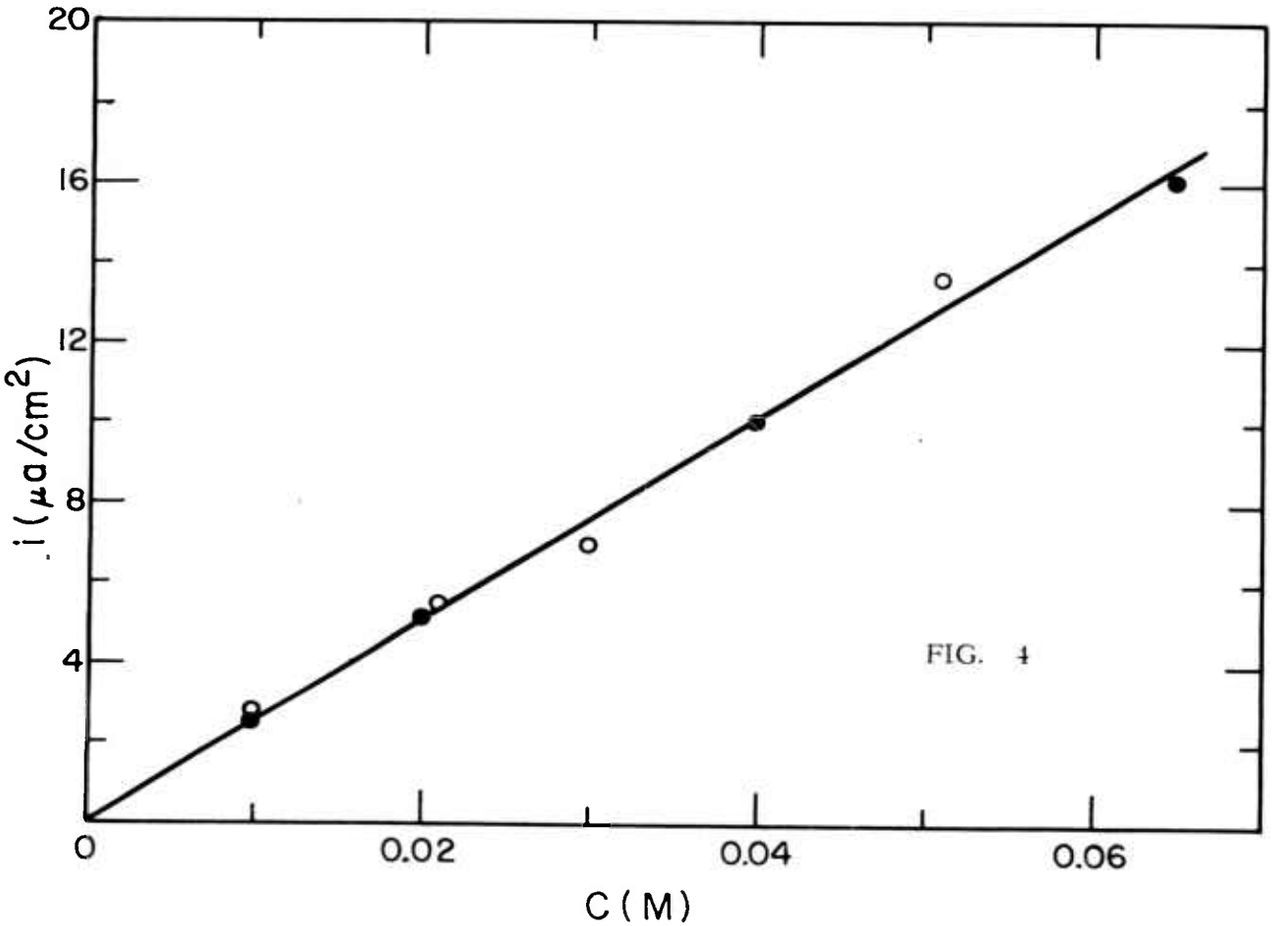

FIG. 4

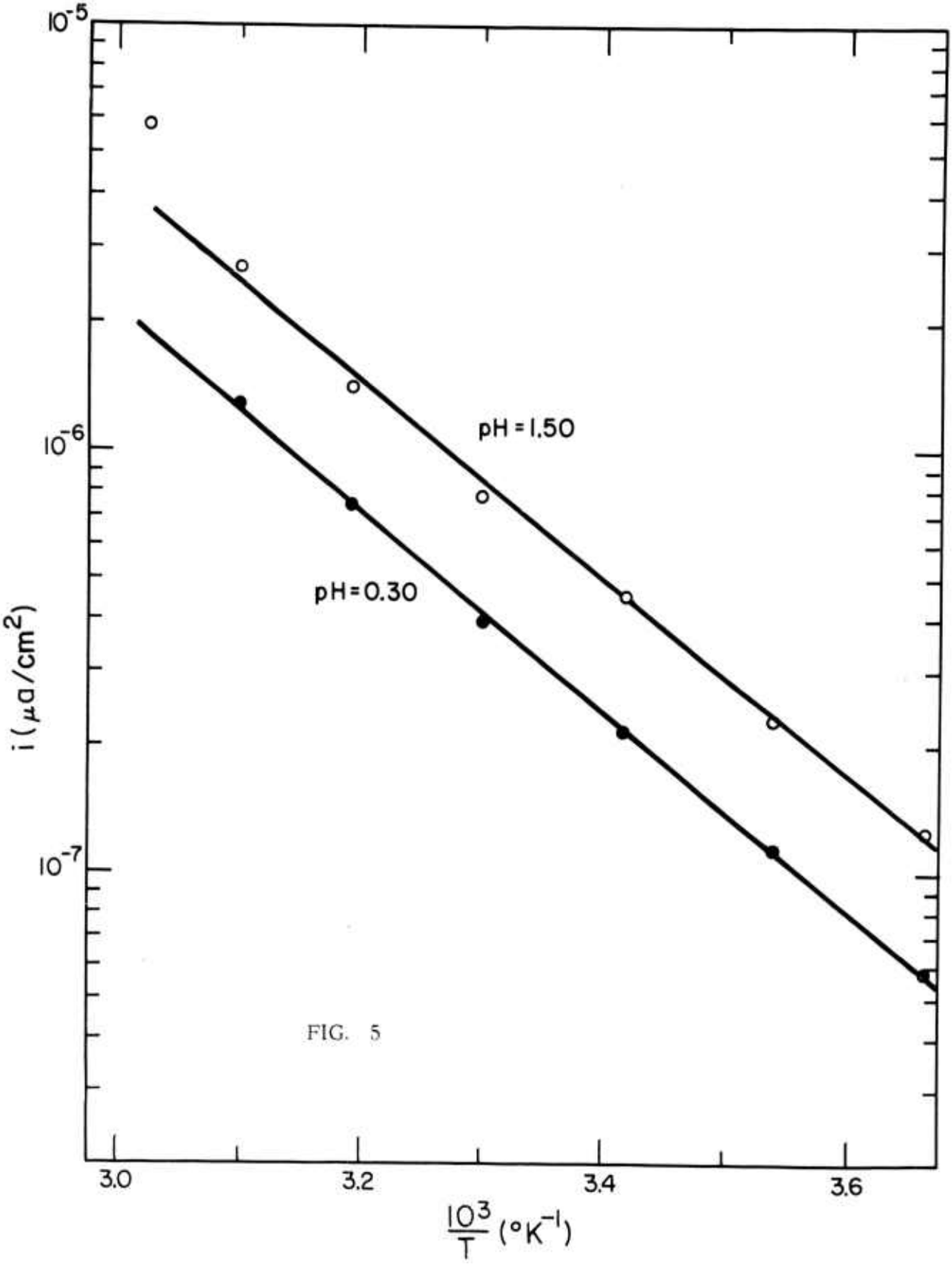

FIG. 5

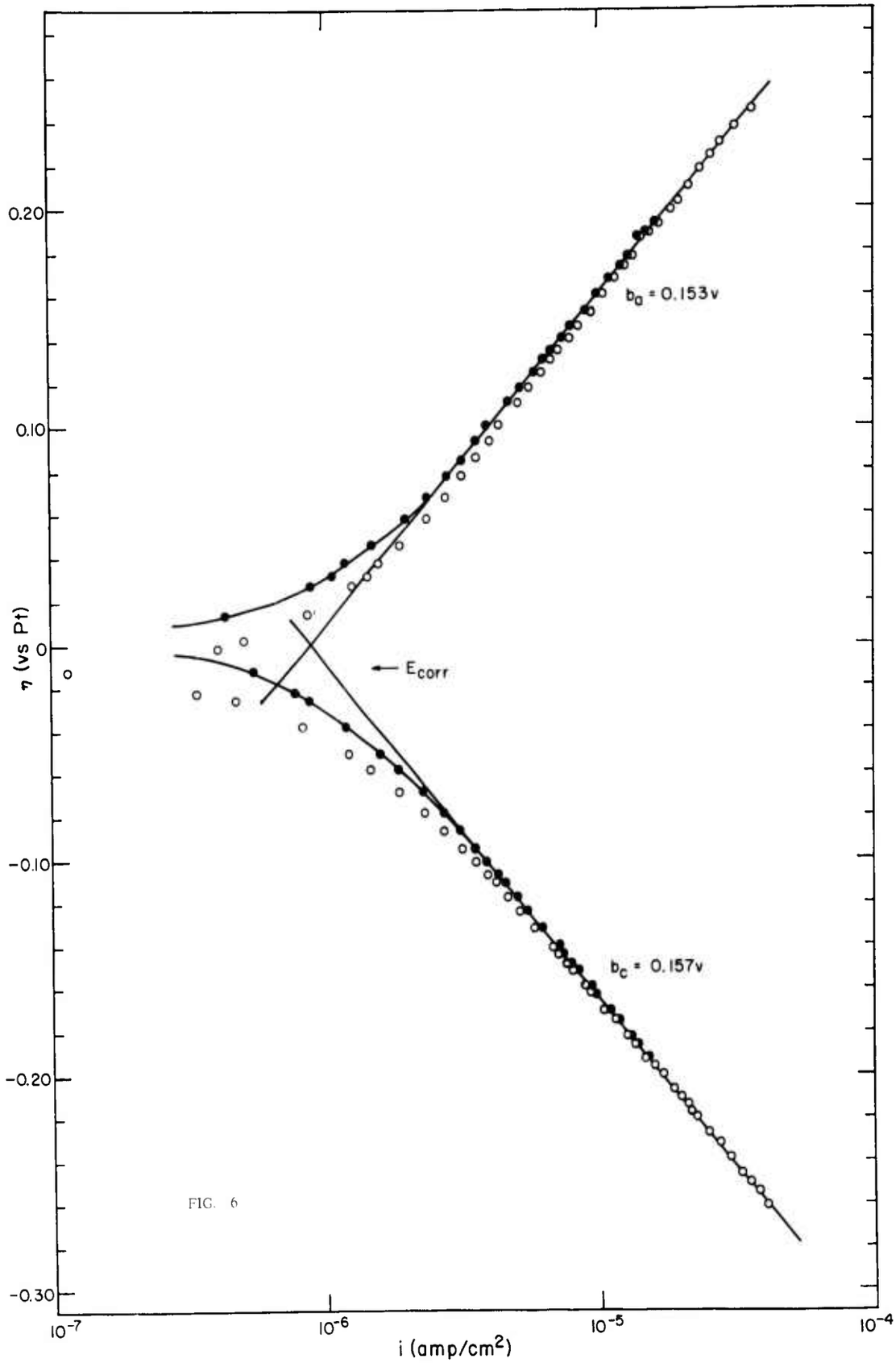
0.20
0.10
0
-0.10
-0.20
-0.30
η (vs Pt)
b_a = 0.153v
E_{corr}
b_c = 0.157v
10^{-7}
10^{-6}
10^{-5}
10^{-4}
i (amp/cm^2)

FIG. 6

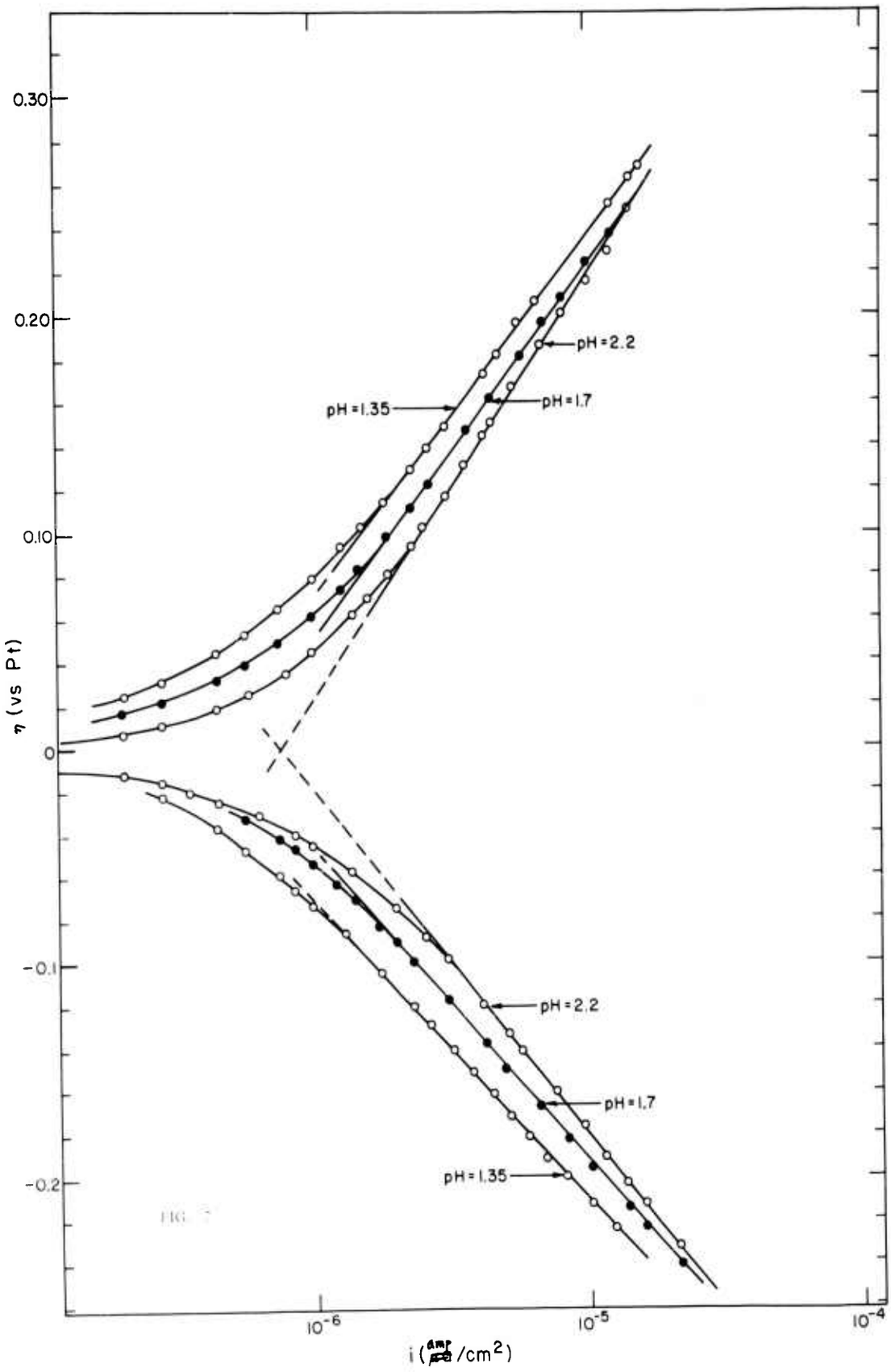
0.30
0.20
0.10
0
-0.1
-0.2
η (vs Pt)
pH = 2.2
pH = 1.7
pH = 1.35
pH = 2.2
pH = 1.7
pH = 1.35
10⁻⁶
10⁻⁵
10⁻⁴
i (amp/cm²)

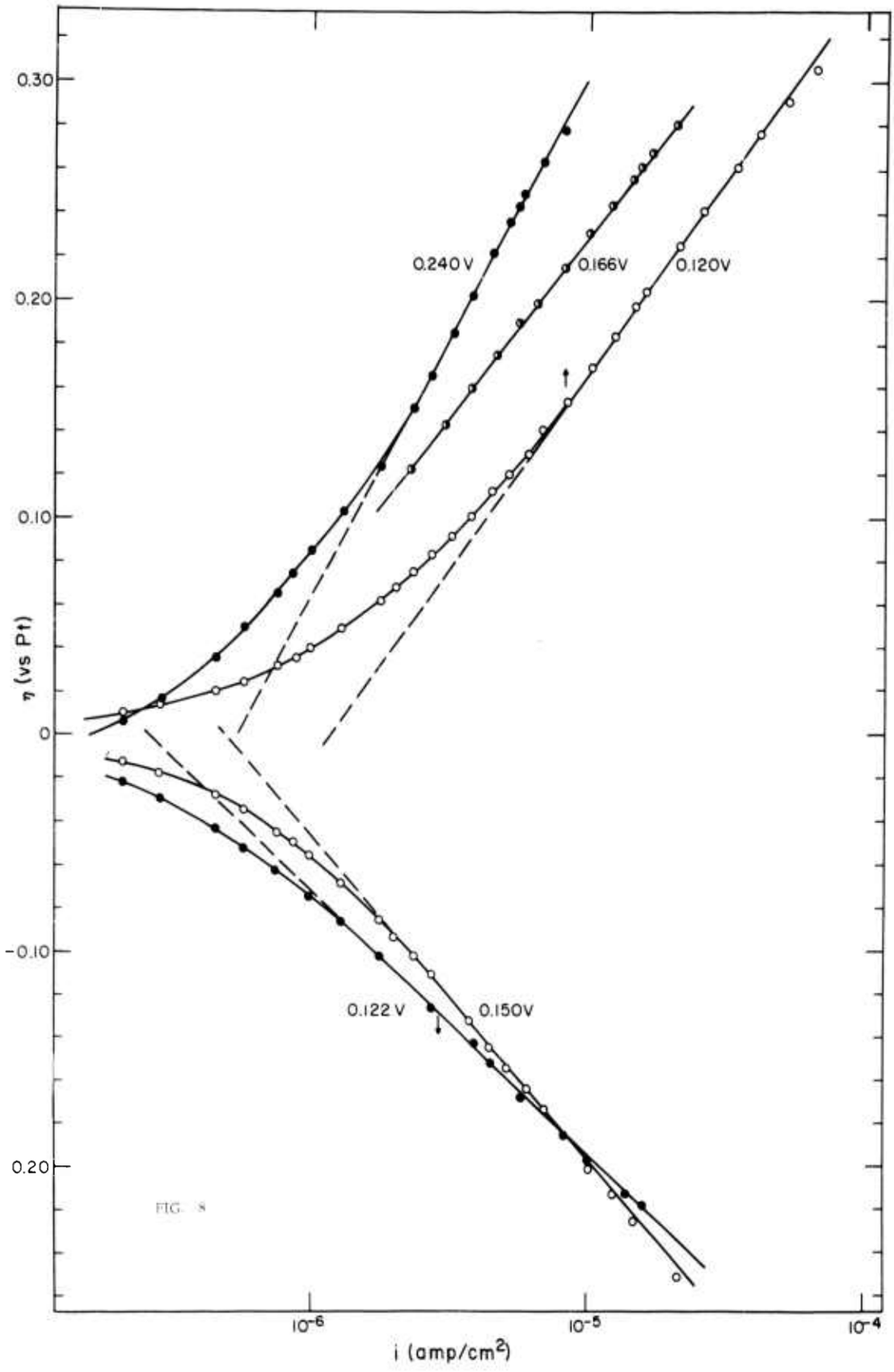
0.30
0.20
0.10
0
-0.10
0.20
η (vs Pt)
0.240 V
0.166V
0.120V
0.122 V
0.150V
10⁻⁶
10⁻⁵
10⁻⁴
i (amp/cm²)

FIG. 8

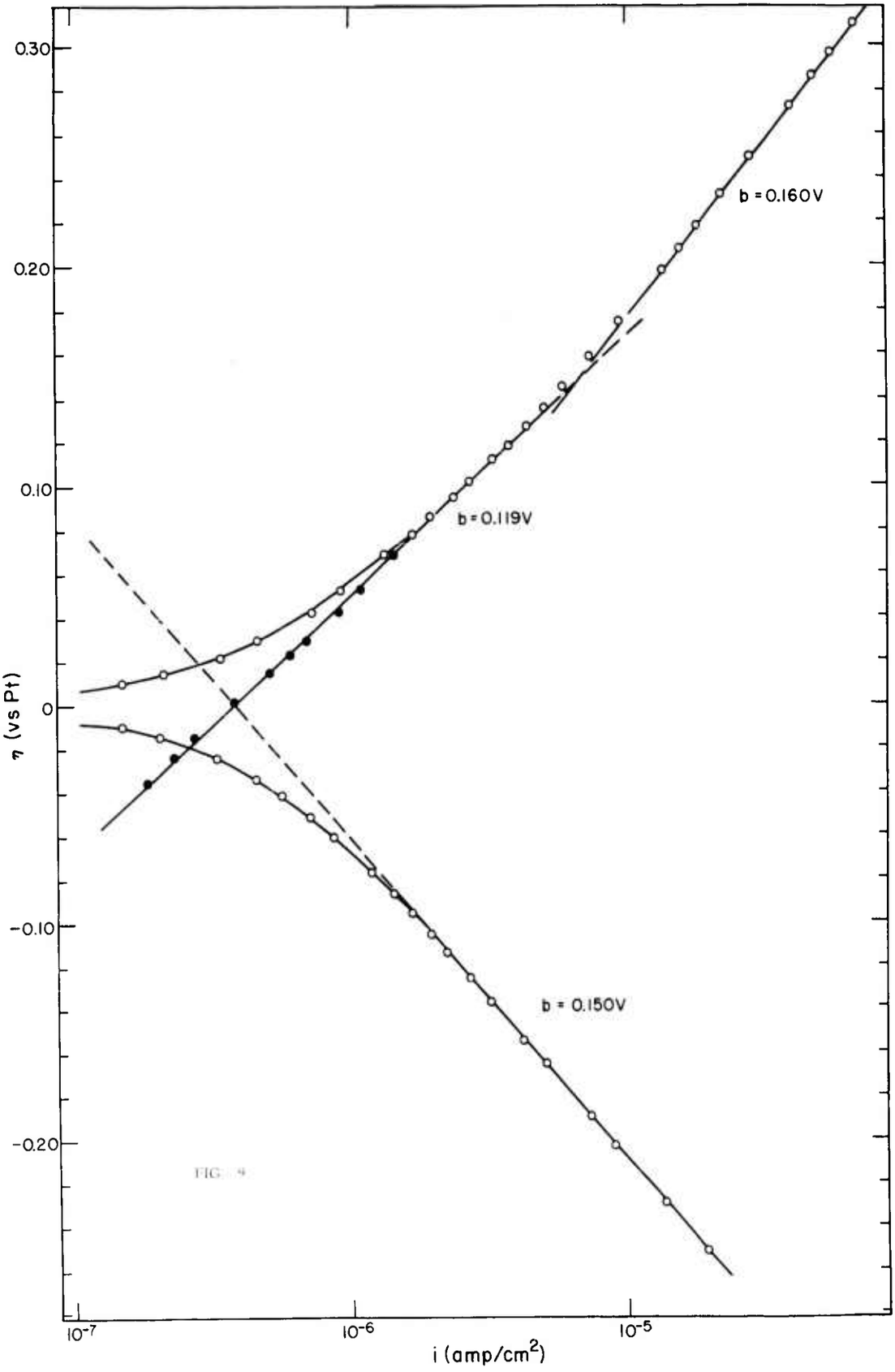
0.30
0.20
0.10
0
-0.10
-0.20
η (vs Pt)
b = 0.160V
b = 0.119V
b = 0.150V
10⁻⁷
10⁻⁶
10⁻⁵
i (amp/cm²)

FIG. 9

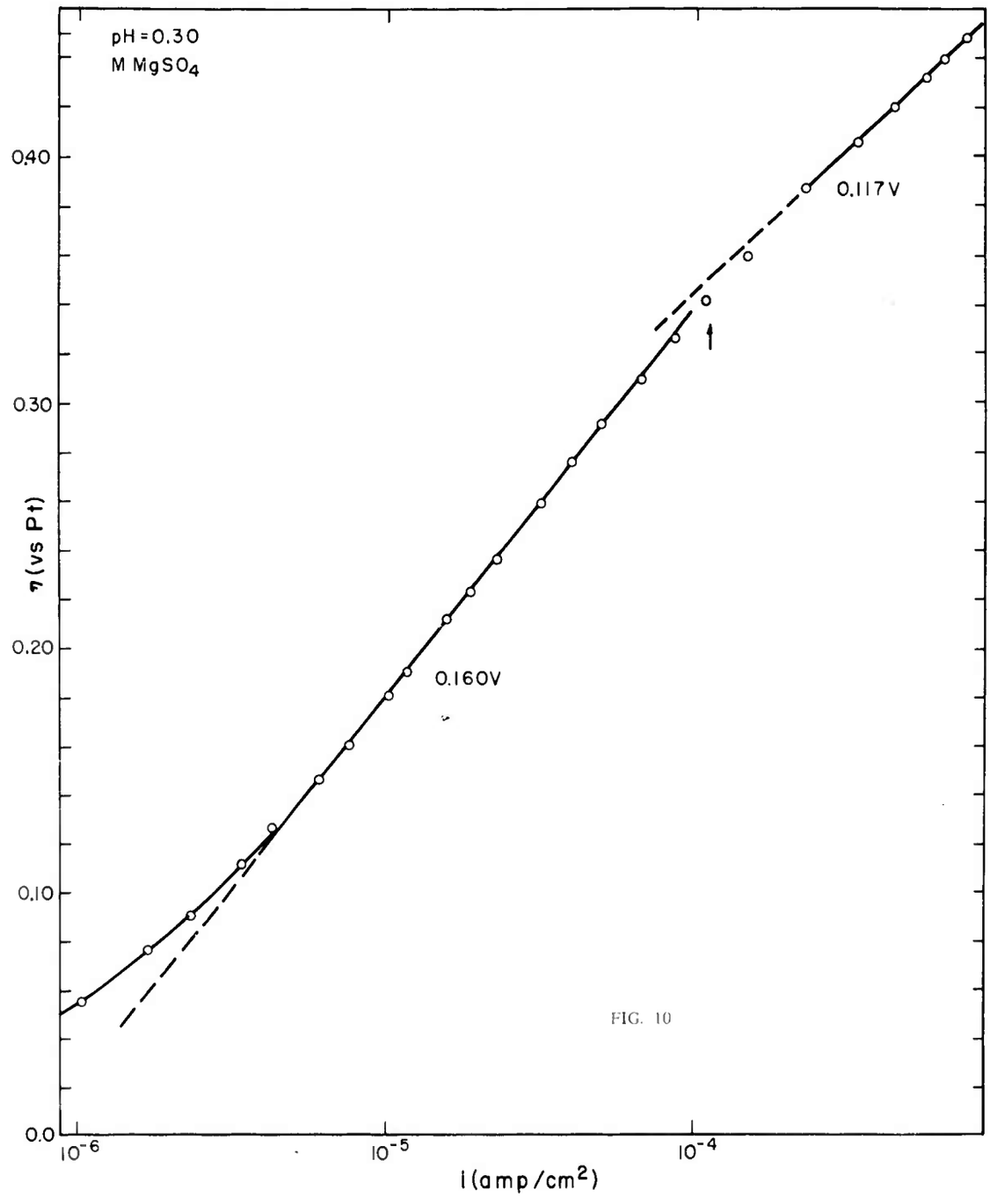
pH = 0.30
M MgSO4
0.40
0.30
0.20
0.10
0.0
η (vs Pt)
0.117V
0.160V
10-6
10-5
10-4
i (amp/cm2)

FIG. 10

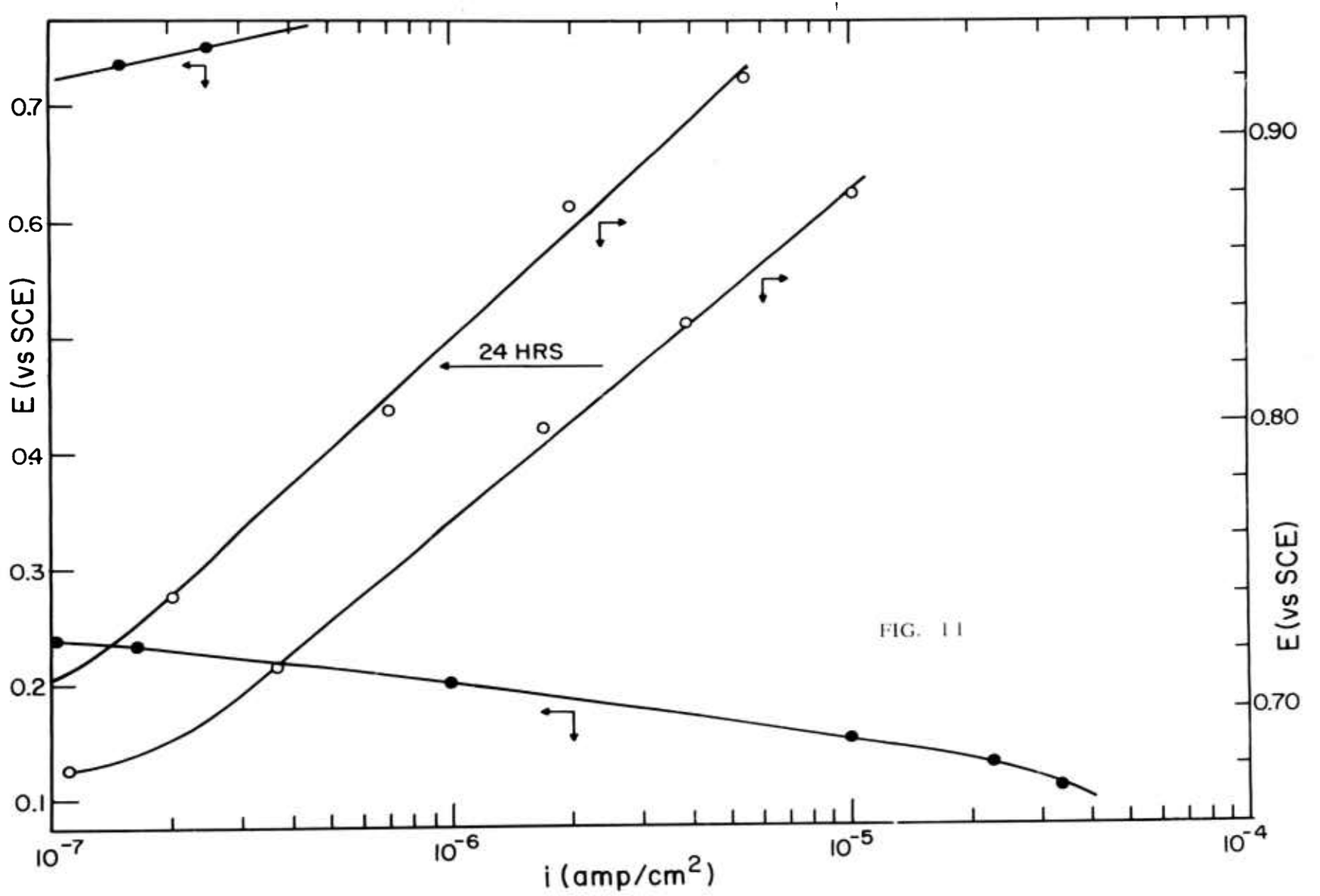
0.7
0.6
0.4
0.3
0.2
0.1
E (vs SCE)
24 HRS
0.90
0.80
0.70
E (vs SCE)
10^{-7}
10^{-6}
10^{-5}
10^{-4}
i (amp/cm^2)

FIG. 11

TECHNICAL REPORT DISTRIBUTION LIST

Contract No. Nonr 3765(00)

Commanding Officer
Office of Naval Research Branch Office
The John Crerar Library Building
86 East Randolph Street
Chicago 1, Illinois (1)

Commanding Officer
Office of Naval Research Branch Office
346 Broadway
New York 13, New York (1)

Commanding Officer
Office of Naval Research Branch Office
1030 East Green Street
Pasadena 1, California (1)

Commanding Officer
Office of Naval Research Branch Office
Box 39 Navy #100 Fleet Post Office
New York, New York (7)

Director, Naval Research Laboratory
Washington 25, D.C.
Attn: Technical Information Officer (6)
Chemistry Division (2)

Chief of Naval Research
Department of the Navy
Washington 25, D.C.
Attn: Code 425 (2)

DDR&E
Technical Library
Room 3C-128, The Pentagon
Washington 25, D.C. (1)

Technical Director
Research & Engineering Division
Office of the Quartermaster General
Department of the Army
Washington 25, D.C. (1)

Research Director
Clothing & Organic Materials Division
Quartermaster Research & Engineering
Command, U.S. Army
Natick, Massachusetts (1)

Air Force
Office of Scientific Research (SRC-E)
Washington 25, D.C. (1)

Commanding Officer
Diamond Ordnance Fuze Labs.
Washington 25, D.C.
Attn: Technical Information Office
Branch 012 (1)

Office, Chief of Research &
Development, Dept. of the Army
Washington 25, D.C.
Attn: Physical Sciences Div. (1)

Chief, Bureau of Ships
Department of the Navy
Washington 25, D.C.
Attn: Code 342C (2)

Chief, Bureau of Naval Weapons
Department of the Navy
Washington 25, D.C.
Attn: Technical Library (4)

ASTIA
Document Service Center
Arlington Hall Station
Arlington 12, Virginia (10)

Director of Research
U.S. Army Signal Research &
Development Laboratory
Fort Monmouth, New Jersey (1)

Naval Radiological Defense
Laboratory
San Francisco 24, California
Attn: Technical Library (1)

Naval Ordnance Test Station
China Lake, California
Attn: Head,
Chemistry Division (1)

Commanding Officer
Army Research Office
Box CM, Duke Station
Durham, North Carolina
Attn: Scientific Synthesis Office (1)

Brookhaven National Laboratory
Chemistry Department
Upton, New York (1)

Atomic Energy Commission
Division of Research
Chemistry Programs
Washington 25, D.C. (1)

Atomic Energy Commission
Division of Technical Information
Extension
Post Office Box 62
Oak Ridge, Tennessee (1)

U.S. Army Chemical Research and
Development Laboratories
Technical Library
Army Chemical Center, Maryland (1)

Office of Technical Services
Department of Commerce
Washington 25, D.C. (1)

Commanding Officer
Office of Naval Research Branch
Office
495 Summer Street
Boston 10, Massachusetts (1)

Director, ARPA
Attn Dr. J. H. Huth
Material Sciences
Room 3D155 The Pentagon
Washington 25, D.C (4)

Dr. S. Schuldiner
Naval Research Laboratory
Code 6160
Washington 25, D. C. (1)

Dr. R.F. Baddour
Department of Chemistry
Mass. Institute of Technology
Cambridge 39, Massachusetts (1)

Inspector of Naval Material
495 Summer Street
Boston 10, Massachusetts (1)

Mr. R.A. Osteryoung
Atomics International
Canuga Park, California (1)

Dr. David M. Mason
Stanford University
Stanford, California (1)

Dr. Howard L. Recht
Astropower, Inc.
2968 Randolph Avenue
Costa Mesa, California (1)

Mr. L.R. Griffith
California Research Corporation
576 Standard Avenue
Richmond, California (1)

Dr. Ralph G. Gentile
Monsanto Research Corporation
Boston Laboratories
Everett 49, Massachusetts (1)

Dr. Ray M. Hurd
Texas Research Associates
1701 Guadalupe Street
Austin 1, Texas (1)

Dr. C. E. Heath
Esso Research & Engineering
Company
Box 51
Linden, New Jersey (1)

Dr. Richard H. Leet
American Oil Company
Whiting Laboratories
Post Office Box 431
Whiting, Indiana (1)

Dr. G. C. Szego
Institute for Defense Analysis
1666 Connecticut Avenue N.W.
Washington 9, D.C. (1)

Dr. Douglas W. McKee
General Electric Company
Research Laboratories
Schenectady, New York (1)

Dr. E. A. Oster
General Electric Company, DECO
Lynn, Massachusetts (1)

Dr. R. R. Heikes
Solid State Phenomena Department
Westinghouse Electric Corporation
Pittsburgh, Pennsylvania

Prof. Herman P. Meissner
Massachusetts Institute of Technology
Cambridge 39, Massachusetts (1)

Mr. Donald P. Snowden
General Atomic
Post Office Box 608
San Diego 12, California (1)

Prof. C. Tobias
Chemistry Department
University of California
Berkeley, California (1)

Dr. Y. L. Sandler
Westinghouse Research Laboratories
Schenectady, New York (1)

Dr. Paul Delahay
Department of Chemistry
Louisiana State University
Baton Rouge, Louisiana (1)

Dr. W. J. Hamer
Electrochemistry Section
National Science Foundation
Washington 25, D.C. (1)

Dr. Herbert Hunger
Power Sources Division
U.S. Army Signal Research &
Development Laboratory
Fort Monmouth, New Jersey

Dr. T.P. Dirkse
Department of Chemistry
Calvin College
Grand Rapids, Michigan (1)

Dr. George J. Janz
Department of Chemistry
Rensselaer Polytechnic Institute
Troy, New York (1)

Mr. N. F. Blackburn
E. R. D. L.
Materials Branch
Fort Belvoir, Virginia (1)

Dr. G. Barth-Wehrenalp, Director
Inorganic Research Department
Pennsalt Chemicals Corporation
Box 4388
Philadelphia 18, Pennsylvania (2)

Dr. B. R. Sundheim
Department of Chemistry
New York University
New York 3, New York (1)

Dr. B. R. Stein
European Research Office
U. S. Army R&D Liaison
Group 985 IDU
APO 757, New York, N.Y. (1)

Dr. E. M. Cohn
NASA
Code RPP
1512 H Street N.W.
Washington 25, D.C. (1)

Dr. E. Yeager
Department of Chemistry
Western Reserve University
Cleveland 6, Ohio (1)

Lockheed Aircraft Corporation
Missiles and Space Division
Technical Information Center
3251 Hanover Street
Palo Alto, California (1)

UNCLASSIFIED